Perturbing an electromagnetic induced transparency within an inhomogeneously broadened transition

E. A. Wilson, N. B. Manson, and C. Wei
Laser Physics Center, Research School of Physical Sciences and Engineering, Australian National University, Canberra ACT 0200, Australia

(Received 4 September 2002; published 25 February 2003)

This paper reports on the effect a perturbing field on an electromagnetically induced transparency. The studies involve inhomogeneously broadened spin transitions of a nitrogen-vacancy color center in diamond and it is observed that the transparency is unaffected, destroyed or split depending on how the perturbing field is coupled to the system. The observations are explained in terms of doubly driven inhomogeneously broadened 4-level systems.

DOI: 10.1103/PhysRevA.67.023812 PACS number(s): 42.50.Gy, 42.50.Hz, 42.62.Fi

I. INTRODUCTION

Electromagnetic induced transparency (EIT) is a well studied phenomenon and has been the subject of numerous publications and review articles [1–3]. EIT is relevant to any 3-level system in a V, Λ, or Ξ geometry, driven by two fields and a typical observation is a transparency or reduction in absorption, where the energy difference (V or Λ system) or sum (Ξ system) of the two fields matches an energy separation within the 3-level system. The transparency occurs through an interference between the absorption pathways. Most of the interest in EIT is for cases where the fields are at optical frequencies, but the phenomenon is general and we have previously reported observation of EIT at radio frequencies associated with spin levels of a nitrogen-vacancy color center in diamond [4]. This spin system is also utilized in the current work because the system exhibits clear EIT and it is simple to introduce additional electromagnetic fields to study how the EIT is affected by a perturbing field. The perturbing field couples one of the three levels to a fourth level. The observations are relevant to other inhomogeneously broadened transitions in solids and Doppler broadened atomic systems with co-propagating beams.

There are a number of applications for EIT such as gain without inversion [6], quantum nondemolition measurements [7], ultraslow light propagation [8], and efficient nonlinear optics [9]. Perturbation of the EIT is of interest as it offers new avenues for controlling these effects [10].

II. SPIN TRANSITIONS IN NITROGEN-VACANCY CENTER IN DIAMOND

The nitrogen-vacancy center in diamond has been reported in previous publications (see Ref. [4]) and only a brief account is given here. The center can be created in any diamond containing single substitutional nitrogen, type 1*b*, by irradiation and annealing. Irradiation with 1 Mev energy creates carbon vacancies and these are mobile at temperatures of 800°C and become trapped at the nitrogen sites to create a trigonal nitrogen-vacancy complex [11]. In crystals with additional nitrogen the complex becomes negatively charged with six unbound electrons [12]. The ground state is an orbital singlet *A* and gives a strongly allowed transition to an orbital doublet *E* with an energy of 1.945 eV [11]. Both ground and excited states have electron spin of $S=1$. Excitation of the $^3A \rightarrow {}^3E$ transition causes a preferential population of the spin levels [13,14] and this spin polarization is considered to arise as a consequence of decay via a singlet level although the details of the process have not been established.

In the present work absorption within the ground spin multiplet at radio frequencies is obtained using the Raman heterodyne technique [15]. This is a coherent optical technique which requires nonzero transition moments between the two ground-state spin levels and a common optical excited state. The selection rules for the *N-V* center does not normally satisfy these conditions as spin is a good quantum number and is conserved in the optical transition. Thus, there will not be optical transitions from different spin levels to a common upper level. However, the selection rules can be relaxed by using a magnetic field to mix the spin states and this is achieved by working close to an avoided crossing of the ground-state spin levels. Then, with the light field resonant with the $^3A \rightarrow {}^3E$ optical transition and the rf resonant with a spin transition, there will be a stimulated Raman signal colinear with the transmitted beam, which can be measured using heterodyne detection. The signal out of phase with the applied rf is proportional to the rf absorption [15] and provides a measure of the electron-spin transitions. The signals are obtained as a beat signal at the frequency of the applied rf field and the responses at one frequency can be distinguished from that of another. Thus, the spectrum of a weak probe can be obtained even when the system is strongly driven by other rf fields.

In the trigonal crystal field the electronic ground state of the nitrogen-vacancy center is split by 2.88 GHz. The $M_S = \pm 1$ levels lie higher in energy and in an axial magnetic field of 1028 gauss the $M_S = -1$ is lowered ($g=2.0028$) and becomes near degenerate with the $M_S = 0$ state (Fig. 1). There is hyperfine structure associated with the nuclear spin of the nitrogen, $I=1$, and the associated parameters are: quadrupole splitting parameter $P=-5.1$ MHz and hyperfine parameter $A\|=2$ MHz, and $A\perp=2.1$ MHz [5]. The off-diagonal Zeeman interaction $g.\underline{B}.\underline{S}$ and hyperfine interaction $A\underline{I}.\underline{S}$ have significant effect when the levels approach and cause a repulsion of levels. Thus, as a function of axial magnetic field in the region of 1028 G there is an avoided crossing of the hyperfine levels as shown in Fig. 1. The experiments are made with the field close to but not exactly at the

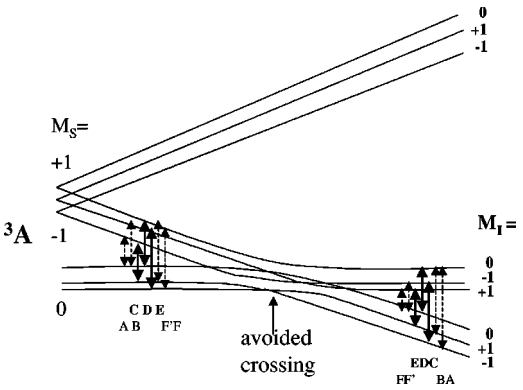

FIG. 1. Ground-state spin levels of the nitrogen-vacancy center given as a function of axial magnetic field.

avoided crossing. The order of the levels is altered but the spectra on the high- and low-field sides of the avoided crossing are simply reversed in energy as indicated in Fig. 1. The energy levels on the low-energy side of the avoided crossing are shown in greater detail in Fig. 2(i). Note the labeling of the nuclear hyperfine levels has been corrected from that given in our previous reports of EIT [4].

The electron-spin transitions are dominated by the three transitions conserving nuclear spin of $M_I=\pm 1,\ 0$. With the mixing of the spin states at the avoided crossing four additional transitions involving the $M_I=0$ levels are induced by off-axis Zeeman and hyperfine interactions. The transitions are shown in Fig. 2(i) and labeled A–F. A schematic of the spectrum is shown below in Fig. 2(ii). The transitions are clearly not to scale and population factors not taken into account. The diagram also indicates the hyperfine transitions and labels these W–Z. The hyperfine transitions are narrow and essentially homogeneously broadened, whereas the electron-spin transitions are inhomogeneously broadened. Figure 2(iii) shows the arrangements of levels and fields used later in this study.

Measurements are made at helium temperatures but it is not the temperature that determines the population in the spin levels. At magnetic-fields values well removed from the avoided crossing, the optical excitation causes a transfers of population from levels involving $M_S=\pm 1$ spins to those associated with the $M_S=0$ state and the populations are independent of nuclear-spin projection. Thus, population is transferred into but not out of the three $M_S=0$ hyperfine levels. Close to the avoided crossing (with good alignment) the hyperfine interaction causes two of the three $M_S=0$ hyperfine levels to be mixed with $M_S=-1$ hyperfine levels leaving only one hyperfine level, $M_S=0$, $M_I=+1$ which is not mixed and, hence, the only state not depopulated by the optical pumping. The result is that with continuous optical excitation the majority of the population is pumped into this one hyperfine level. Below the avoided crossing this is the lowest level and, thus, the population is equivalent to that obtained with thermal relaxation at very low temperatures. However, it is important to realize that it is optical pumping that determines the populations and the relaxation rates. The relaxation processes, therefore, are not changed by the order of the levels and there is a one-to-one correlation of the

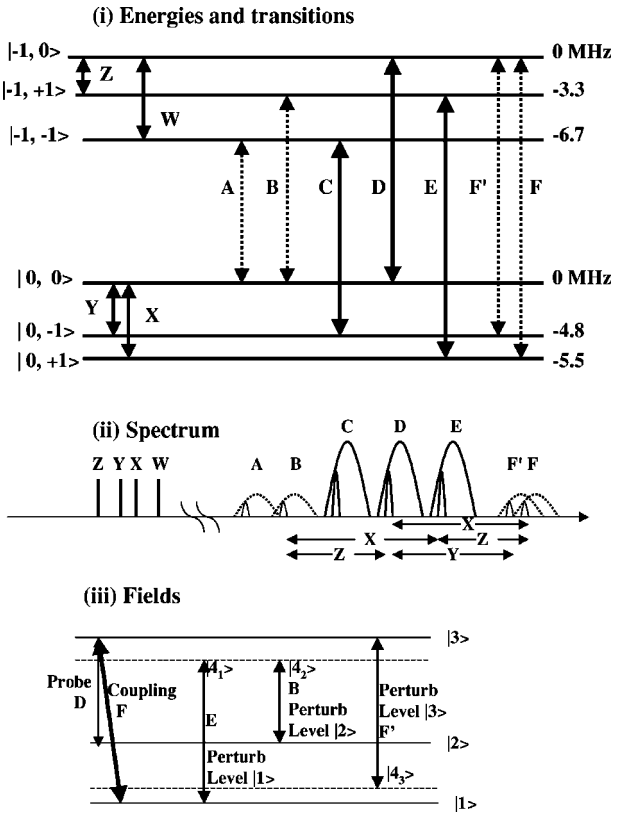

FIG. 2. (i) Energy levels and transitions used in the experiments. A typical separation between the three upper and three lower spin levels is 40 MHz. The figure also gives the notation for the transitions. (ii) Indication of relative frequency and strength of the spin transitions. The inhomogeneously broadening in the electron-spin transitions are indicated. The hyperfine transitions are homogeneously broadened. The population factors are not taken into account. (iii) Energy levels used in the study. The Λ system is formed by levels $|1\rangle\equiv|0+1\rangle$, $|2\rangle\equiv|0,0\rangle$, and $|3\rangle\equiv|-1,0\rangle$. The coupling field drives the $|1\rangle$–$|3\rangle$ transition and the $|2\rangle$–$|3\rangle$ is probed. In perturbing the EIT three cases are studied with level $|1\rangle$, $|2\rangle$, or $|3\rangle$ coupled to a forth level as indicated.

behavior above and below crossing. Above crossing the largest populated level will not be the lowest level. However, even though experiments involve fields above and below the avoided crossing we present all discussion in terms of the situation below the avoided crossing where the majority of the population is in the lowest-energy level.

In the experimental arrangement the $1\times1\times1$ mm^3 diamond crystal is cooled to liquid helium temperature within the bore of a superconducting magnet. The magnet applies a horizontal dc field of 1000 G along a $\langle 111\rangle$ direction and along the axis of the nitrogen-vacancy center of interest. The light propagates along a $\langle 110\rangle$ direction at right angles to the field and is vertically polarized. The frequency of the light is in resonance with the $^3A\rightarrow{}^3E$ zero-phonon line at 1.945 eV. The axis of the rf coil is likewise along the $\langle 110\rangle$ direction and at right angles to the center of interest. An rf field from a network analyzer is amplified and applied to the coil (for weak field $B_{rf}<0.01$ G). The resultant beat signal on the transmitted light is detected by a pin diode and applied to the input of a network analyzer. Under these conditions a Raman

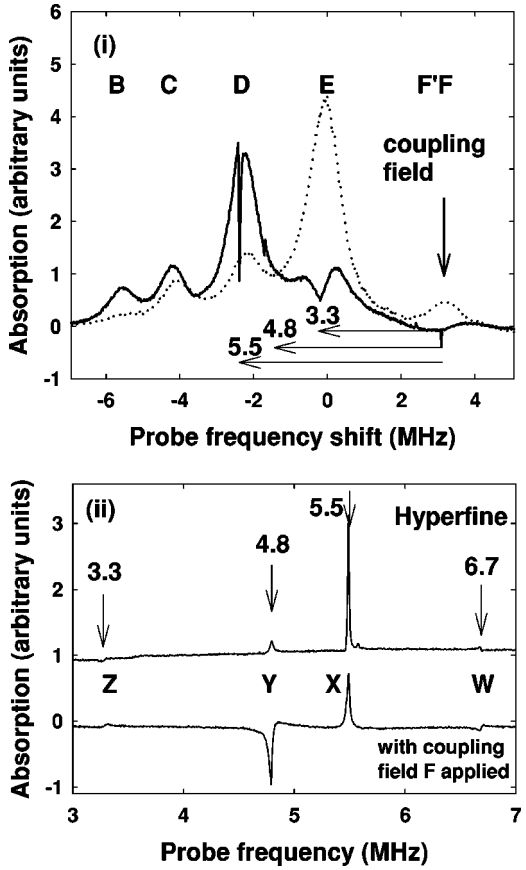

FIG. 3. (i) Electron-spin absorption spectrum obtained by Raman heterodyne detection. Obtained for a field of 1018 G aligned along the $\langle 111 \rangle$ direction and the origin is at 40 MHz. For the dashed trace there are no driving fields present whereas for the solid line a field is applied at a frequency of 3.3 MHz. (ii) The hyperfine absorption spectrum taken under the same conditions as (i) with and without coupling field.

heterodyne signal in the range 0–100 MHz is obtained and the signal used to further improve the experimental conditions. For example, the alignment of the crystal can be improved by minimizing the frequency for a fixed dc magnetic field. Also the dc field may be subsequently varied to adjust the separation of the spin levels. A spectrum with the separation of the spin levels adjusted to 40 MHz is shown as a dashed line in Fig. 3(i). There are three allowed transitions, *C*, *D*, and *E* and the *E* transition dominates the spectrum due to the majority of the population being in the one hyperfine level. A weaker transition, *F* also originates from the populated level and is clearly observed. The hyperfine transitions can be measured under the same condition and is shown in the upper trace in Fig. 3(ii).

III. ELECTROMAGNETICALLY INDUCED TRANSPARENCY IN THE ELECTRON SPIN TRANSITION

EIT involves three levels and the phenomenon can be illustrated using (almost) any three of the six levels in Fig. 2(i). Without loss of generality the study is restricted to one EIT example, and for the example we chose to probe the allowed transition *D* with the coupling field resonant with a weakly allowed transition, *F* [Fig. 2(iii)]. The spectrum is significantly different depending on whether the coupling field is applied or not (Fig. 3). For example, driving the *F* transition transfers population from the $M_S=0$, $M_I=+1$ ground state to the $M_S=0$, $M_I=0$ level and this results in a decrease in the *E* absorption and an increase in the *D* absorption. Also in the hyperfine spectrum the strength of the 5.5 MHz ($M_I=+1 \rightarrow M_I=0$) absorption is decreased and the 4.8 MHz ($M_I=-1 \rightarrow M_I=0$) transition occurs with gain. More significantly, however, for the present study is the occurrence of the central dip due to EIT in the *D* absorption band 5.5 MHz from the frequency of the coupling field. The strong field has another effect in that it is resonant with the wing of the inhomogeneously broadened F' transition. The field again acts as a coupling field and accounts for the weak EIT in the side of the *D* transition 4.8 MHz from the frequency of the coupling field (Fig. 3).

Parameters associated with this EIT can be obtained from the spectrum and from independent measurements. For example, the inhomogeneous linewidth (1 MHz) of the spin transitions, *F* and *D*, are obtained directly from the spectrum in Fig. 3(i), whereas the homogeneous linewidth can be inferred from the decay of two pulse spin echoes. Echoes have been reported in a previous study and they give a homogeneous linewidth of 60 kHz [4]. The linewidth is reasonably independent of the magnetic field and this value is valid here. The diagonal relaxation rates have been obtained from spin recovery and are of the order of 30 kHz. [16]. The parameters of the hyperfine transition, Y, are also required and these are likewise determined from Raman heterodyne measurements. The linewidth can be obtained from the spectrum shown in Fig. 3(ii). It has a value of 10 kHz. In this case the linewidth does depend on the setting of the dc magnetic field and the values are very different from those reported previously for alternative values of magnetic field [4]. However, the previous studies showed that the inhomogeneous broadening was only a few kHz, and the small inhomogeneous broadening will be neglected in this work. The hyperfine lifetimes are long (seconds) and are not critical for the calculations.

The strengths of fields driving an allowed transition (for example, *D*) can be determined from the frequency of nutation obtained when gating on a resonant rf field. The Rabi frequency is determined for one rf power value and other values obtained by scaling. Establishing the strength of the fields driving the weaker transitions such as *F* could not be determined in this way. However, the transitions have an absorption ≈ 0.17 of an allowed transition (e.g., *F* compared with *E*) and assuming the Rabi frequencies scale it enables us to establish the Rabi frequency from knowledge of driving an allowed transition. This is not entirely satisfactory and some uncertainty could result. Throughout the values have not been determined with high accuracy but it will be shown that they are sufficient to establish the origin of the observed phenomenon.

IV. CALCULATION OF ELECTROMAGNETIC INDUCED TRANSPARENCY

With the knowledge of the parameters of the system, the EIT in an inhomogeneous line can be calculated by solving

the density matrix equations. The EIT normally involves two fields and 3-levels but as there is an intention of introducing another field and another level the equations are given for the 4-level case:

$$\rho_{11}=\gamma_{14}\rho_{44}+\gamma_{13}\rho_{33}+\gamma_{12}\rho_{22}-i\Omega_{coup}(\rho_{31}-\rho_{13}),$$

$$\rho_{22}=\gamma_{24}\rho_{44}+\gamma_{23}\rho_{33}-\gamma_{12}\rho_{22}+\gamma_{21}\rho_{11}-i\Omega_{probe}(\rho_{32}-\rho_{23}),$$

$$\rho_{33}=-\gamma_{34}\rho_{33}-\gamma_{13}\rho_{33}-\gamma_{23}\rho_{33}-i\Omega_{coup}(\rho_{31}-\rho_{13})-i\Omega_{probe}(\rho_{32}-\rho_{23}),$$

$$\rho_{44}=-\gamma_{24}\rho_{44}-\gamma_{14}\rho_{44}+\gamma_{34}\rho_{33}+i\Omega_{pert}(\rho_{24}-\rho_{42}),$$

$$\dot{\rho}_{12}=-(\Gamma_{12}+i\Delta_{12})-i\Omega_{coup}\rho_{23}-i\Omega_{probe}\rho_{13}-i\Omega_{pert}\rho_{41},$$

$$\dot{\rho}_{13}=-(\Gamma_{13}+i\Delta_{13})\rho_{13}-i\Omega_{coup}(\rho_{11}-\rho_{33})-i\Omega_{probe}\rho_{12},$$

$$\dot{\rho}_{14}=-(\Gamma_{14}+i\Delta_{14})-i\Omega_{pert}\rho_{12}-i\Omega_{coup}\rho_{43},$$

$$\dot{\rho}_{23}=-(\Gamma_{23}+i\Delta_{23})\rho_{23}-i\Omega_{probe}(\rho_{22}-\rho_{33}-i\Omega_{pert}\rho_{43}-i\Omega_{coup}\rho_{21},$$

$$\dot{\rho}_{24}=-(\Gamma_{24}+i\Delta_{24})\rho_{24}-i\Omega_{pert}(\rho_{22}-\rho_{44})-i\Omega_{pert}\rho_{34},$$

$$\dot{\rho}_{34}=-(\Gamma_{34}+i\Delta_{34})\rho_{34}-i\Omega_{pert}\rho_{32}-i\Omega_{probe}\rho_{42}-i\Omega_{coup}\rho_{41},$$

where

$$\Delta_{12}=\Delta_{coup}-\Delta_{probe},\ \Delta_{14}=\Delta_{coup}-\Delta_{pert}-\Delta_{probe}\ \text{and}\ \Delta_{34}=\Delta_{pert}-\Delta_{probe}.$$

γ_{ij} are the population decay rates from level i to j and Γ_{ij} are the dephasing rates of the transition between levels i and j. The Rabi frequency and detunings of the probe, coupling and perturbing field are denoted by $\Omega_{probe},\Delta_{probe}$, $\Omega_{coup},\Delta_{coup}$, and $\Omega_{pert},\Delta_{pert}$, respectively. To calculate the 3-level case we set $\rho_{44}=0$ and $\gamma_{34}=0$.

As discussed above, the parameters have been measured under similar but not identical conditions and the measurements are used to provide an estimate of the values for the calculation. Some of the rates will have similar values and are taken as equal. For example, the electron-spin population decay is taken to be 60 kHz for all the hyperfine components and a uniform branching ratio of 4:1 is taken for the nominally allowed to nominally forbidden hyperfine transitions. The population transfer between hyperfine levels is long and estimated at 1 Hz although the precise value is not critical. The dephasing rates of the electron spin transitions are taken to be 60 kHz, independent of hyperfine component and the dephasing rate of the hyperfine transitions are estimated at 10 kHz. These are summarized in Fig. 4.

The equations are solved for ρ_{23} as a function of probe detuning to first order in Ω_{probe} and the imaginary part gives the absorption spectrum of a weak probe field. The calculation is repeated for various transition frequencies corresponding to different centers within the inhomogeneous distribution and such results are shown in Fig. 5. The spectrum associated with individual homogeneous lines are displaced for clarity and these are added (assuming a Gaussian distribution in strength) to give the absorption of an inhomogeneous distribution. For this calculation the strength of the coupling field is taken to be $\Omega_{coup}=70$ kHz and with the above parameters gives minor broadening from the hyperfine limit of 10 kHz to 15 kHz. The depth of the transparency is 60%. The situation is considered to be in good correspondence with experiment although a 60% depth is obtained with a marginally lower Rabi frequency of 60 kHz and the inaccuracy is probably due to imprecise parameters.

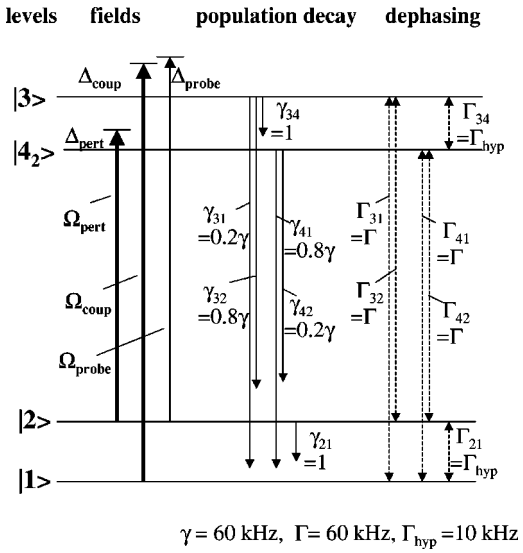

FIG. 4. Notation and parameter values used in the 4-level calculation, where an EIT is perturbed by an additional field. The arrows on the right indicate the three fields; coupling, perturbing, and probe. The Rabi frequencies are denoted by Ω_i and the detunings by Δ_i. Values of the relaxations are given at the bottom.

V. PERTURBATION OF ELECTROMAGNETICALLY INDUCED TRANSPARENCY: SHARED LEVEL, $|3\rangle$

The interest of the current study is to investigate how EIT (involving three levels and two fields) is affected by a further electromagnetic field (giving four levels and three fields). Three situations will be considered and are distinguished by which of the three levels, $|1\rangle$, $|2\rangle$, or $|3\rangle$ is perturbed [see Fig. 2(iii)]. Note in each case the additional field is resonant with an inhomogeneously broadened transition. For each case the approach is to first give a qualitative discussion of the situation. It is assessed whether the effect of introducing a particular perturbing field can be anticipated. The experimental results are then given and if they match prediction decided whether there is benefit of detailed modeling. Conclusions are drawn before proceeding to consider an alternative perturbing field.

The first case to be considered is, where the additional field couples the shared level $|3\rangle$ to a fourth level, denoted $|4_3\rangle$ [Fig. 2(iii)]. In this geometry the perturbing field has effects on the shared level but there is no first-order effect on

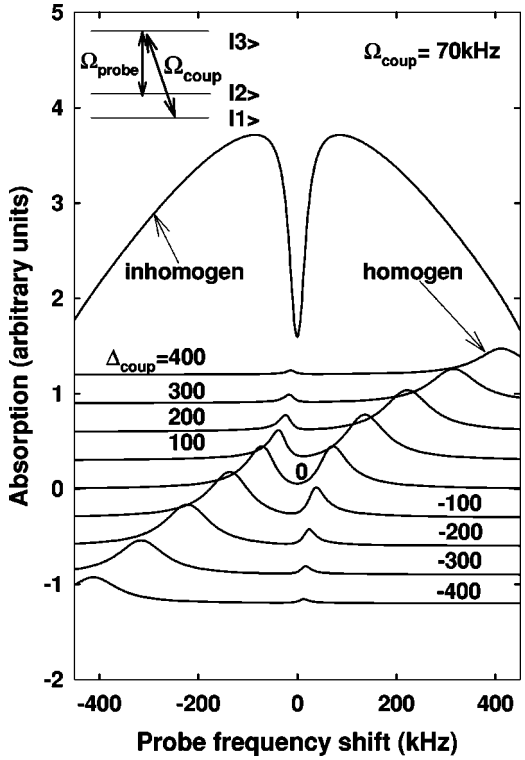

FIG. 5. EIT calculated for an inhomogeneously broadened 3-level system. The parameters of the system are given in the text. The lower traces show the response of individual homogeneously broadened components for a driving field with a Rabi frequency of 70 kHz. The upper trace gives the sum assuming a Gaussian distribution with a linewidth of 1 MHz.

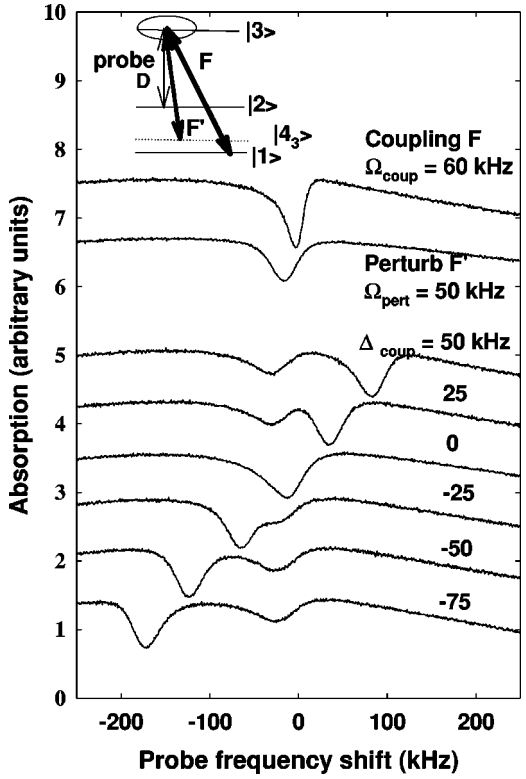

FIG. 6. A series of measurements showing the effect on an EIT feature, where a field F' perturbs the level common to coupling and probe fields as shown in the insert. The uppermost trace indicates the spectrum of a probe beam swept in frequency through the D transition when only the coupling field F is applied. The second trace shows the response when only the perturbing field F' is applied. In the lower traces both of the above driving fields are present and the separate traces are obtained with the coupling field shifted in frequency units of 25 kHz as indicated.

the narrow $|1\rangle \rightarrow |2\rangle$ transition. As a consequence it is anticipated that the sharp EIT associated with coupling and probe fields will be still be observed. The difference is, however, that the perturbing field can act also as a coupling field for a different 3-level system. Some of the levels and fields are coincident with those of the initial 3-level system and the same transition is probed. Consequently it is predicted that there will be two independent EIT features in the probed transition. Two transparencies within an absorption is consistent with three separate absorptions as obtained in a previous publication involving a doubly driven 3-level system probed to a fourth level [17]. When inhomogeneous broadening is included the situation is not fundamentally changed and two EIT features will be present. Thus, from preliminary considerations it is concluded that the initial EIT will not be significantly modified by the introduction of the second driving field i.e., there will be two EIT features and the two will not interfere in first order.

The experimental observation of this situation is shown in Fig. 6. The levels involved are shown in the insert. The primary EIT considered is the same as that shown in Fig. 3. A probe field is swept through the D transition with the coupling field applied to the F transition 5.5 MHz higher in frequency. The perturbing field is resonant with the F' transition 4.8 MHz higher in frequency. It can be seen that the effect of the perturbing field is to introduce a second EIT near the peak of the D absorption. The experiments also show that the presence of this second EIT has little effect on the initial EIT (Fig. 6). The two upper traces in Fig. 6 give the transparencies for the coupling and perturbing field applied independently whereas in the lower traces both driving fields are present. The frequency of the coupling field is varied from trace to trace and changes the position of one of the EIT features. With both fields present the transparencies are simply superimposed with some minor broadening and some reduction in depth when the transparencies coincide. The broadening is due to off resonant pumping, i.e., perturbing field, ideally driving F', also driving F and vice versa.

It is concluded that for this geometry the observations are in general agreement with the prediction in that the second field has little effect on the initial EIT. The phenomenon is not considered to be of sufficient novelty to merit detailed modeling.

VI. PERTURBATION OF ELECTROMAGNETICALLY INDUCED TRANSPARENCY: COUPLING LEVEL, $|1\rangle$

The second case considered is where level $|1\rangle$ is coupled to a fourth level, $|4_1\rangle$ [see Fig. 2(iii)]. Rather than considering the perturbation of an EIT this geometry is better consid-

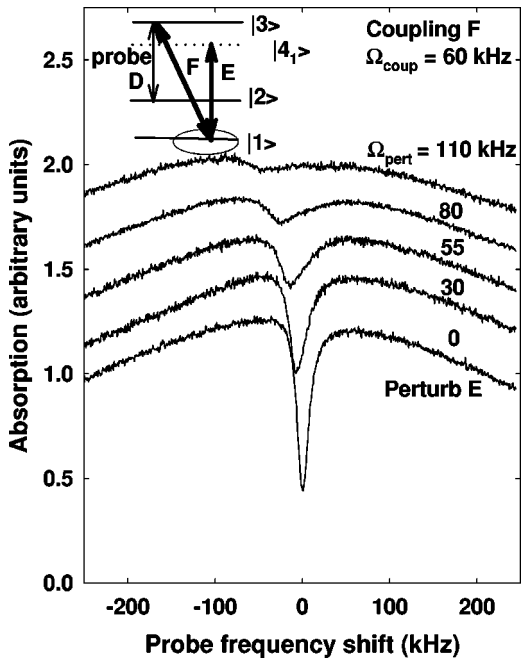

FIG. 7. A series of measurements showing how an EIT feature is effected by a field *E* perturbing the coupling level. The levels and fields are indicated in the insert. The lowest trace gives the spectrum when only the coupling field is applied. For the other traces the perturbing field is applied simultaneously and its strength is indicated on the right.

ered as a doubly driven system probed to a fourth level. A situation considered previously [17]. For example, levels $|1\rangle$, $|3\rangle$, and $|4_1\rangle$ give a 3-level system with two strong driving fields and this is monitored by probing to level $|2\rangle$. From this previous work it can be predicted that the fields will give rise to a splitting into a three line pattern. However, inhomogeneous broadening has the effect of varying the frequency of the three lines associated with the contributing centers such that there will be no structure when the contributions are summed. Based on the above considerations it is predicted that the perturbing field will lead to a loss of the transparency.

The experimental results are shown in Fig. 7. The EIT is obtained as previously by sweeping through the inhomgeneously broadened *D* transition with a coupling field applied near the peak of the weaker *F* transition 5.5 MHz higher in frequency. The perturbing field is resonant with the *E* transition. When the perturbing field is increased from a Rabi frequency of 0 kHz to 110 kHz the EIT is broadened and the depth is reduced. The small shift in the average frequency of the EIT is due to the pertubing field, ideally driving *E,* also driving both *F* and *D* off resonance. The major effect of the perturbing field is the loss of the EIT consistent with the description given above. The effect is again not of sufficient interest to merit a presentation of a detailed analysis.

A similar arrangement of fields has been studied by Echaniz *et al.* [18] for a homogeneously broadened Rb system and by Ye, Zibrov, and Rostovtsev [19] for a Doppler broadened Rb atomic system. Echaniz *et al.* observed the predicted three level pattern. With Doppler broadening Ye, Zibrov, and Rostovtsev [19] found that for counter propagating beams the three line spectrum of the doubly driven system were positioned symmetrically about zero frequency for each velocity group. As a consequence in this geometry a minima is obtained on either side of a central absorption and an apparent splitting of the EIT. For copropagating beams the different velocity groups give a shift in frequency of the three lined spectrum for the doubly driven system and correspondingly no distinctive spectral feature was obtained in the experiment. This latter case is similar to the situation in a solid and no transparency is obtained with perturbing field applied.

We have also reported the situation where $|4_1\rangle$ is another hyperfine level of the ground spin level [20]. In contrast to the present situation the $|1\rangle \rightarrow |4_1\rangle$ transition is both narrow and near homogeneous. With no inhomogenous broadening in the driven transition the frequency of the features of the contributing centers coincide and, hence, will also occur in the inhomogeneously broadened $|2\rangle \rightarrow |3\rangle$ probed transition. Thus, when the perturbing field drives the hyperfine transition the EIT is split without any significant increase in linewidth [4]. This case provides an excellent example of a double dark resonance proposed for atomic systems [10].

VII. PERTURBATION OF ELECTROMAGNETICALLY INDUCED TRANSPARENCY: PROBE LEVEL, $|2\rangle$

The rest of the paper is concerned with the third case, where the fields are as indicated on the right in Fig. 2(iii). The perturbing field couples the ''probe'' level to a fourth level denoted $|4_2\rangle$. The perturbing field can again acts as a ''coupling'' field and a sharp transparency might be expected. However, such a transparency is not the dominant feature. The dominant feature is a broad spectral hole and the presence of the hole has a surprisingly large effect on the characteristics of the spectrum. Thus, our preliminary consideration in this case does not anticipate our observations and will not be given in any detail.

Experimentally the EIT is created as in all previous cases by applying a coupling field resonant with the weakly allowed *F* transition and observed by probing the *D* transition (insert in Figs. 8 and 9). In this case the perturbing field is applied resonant with a second weakly allowed transition *B* displaced 3.3 MHz to lower energy of the *D* transition. What occurs is well illustrated by the spectrum shown in Fig. 3. The coupling field gives rise to the EIT in *D* but also gives a broad transparency feature in *E*. The broad feature is a spectral hole. A new field or perturbing field applied to *B* gives the reverse. It gives a broad transparency, spectral hole, within the *D* transition and a sharp EIT within the inhomogeneously broadened *E* transition. When both fields are applied holes and EIT overlap and what we are interested in is the behavior of the interaction of the broad hole and the narrow EIT.

The results of a series of studies are shown in Figs. 8 and 9. For Figs. 8(i) and 8(ii) the coupling field is tuned to the peak of the *F* transition and the perturbing field to the peak of the *B* transition and this gives a EIT and hole coincident at the peak of the *D* transition. For Fig. 8(i) the coupling field is fixed in frequency and strength ($\Omega_{coup} = 60$ kHz), whereas

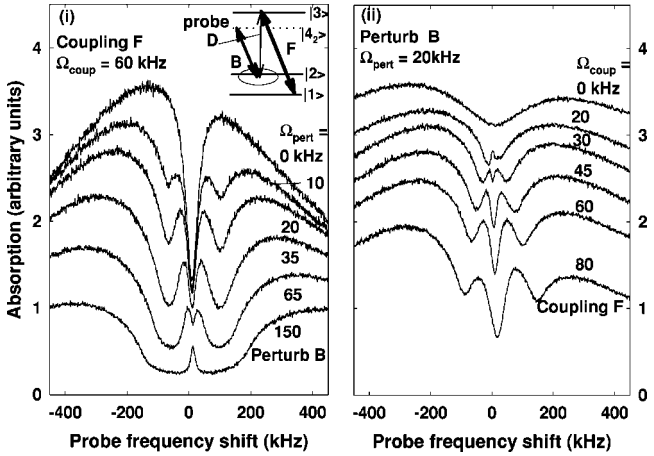

FIG. 8. A series of measurements showing the effect on an EIT feature where a field perturbs the probe level. The levels and fields used are shown in the insert. In (i) the coupling field is fixed in frequency and strength. The perturbing field is adjusted in frequency to give a hole coincident with the EIT and the strength is varied between 0 and 150 kHz as indicated. In (ii) the perturbing field is fixed in frequency and strength whereas the strength of the coupling field is varied. One trace, with $\Omega_{coup}=60$ kHz, and $\Omega_{pert}=20$ kHz, is common and also given in Fig. 9.

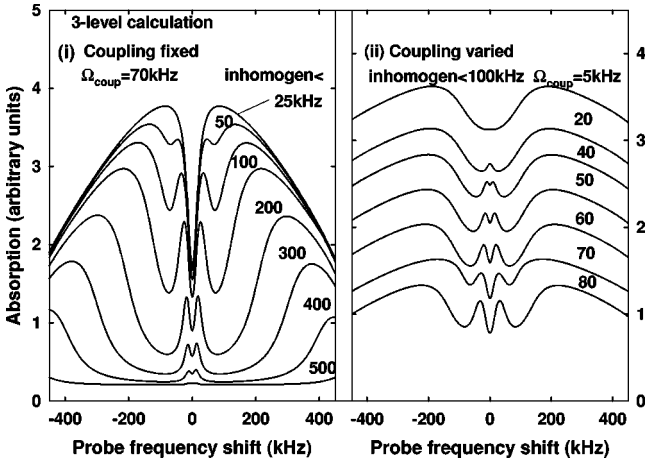

FIG. 10. Calculation of EIT in an inhomogeneous 3-level Λ system as for Fig. 5 except some contributions are eliminated. (i) The top trace is equivalent to that given in Fig. 5. In the lower traces the central components within the inhomogeneous line are excluded in the sum and the range excluded is indicted on the right. (ii) Contributions of centers with resonant frequencies within 100 kHz of zero detuning are eliminated from the calculation of EIT in an inhomogeneously broadened line. The strength of the coupling field is indicated.

the strength of the perturbing field is varied from top trace, with a strength of $\Omega_{pert}=0$ kHz to bottom trace with $\Omega_{pert}=150$ kHz. The alternate driving field is varied in Fig. 8(ii); the perturbing field is fixed at $\Omega_{pert}=20$ kHz and the coupling field varied from $\Omega_{coup}=0$ to $\Omega_{coup}=80$ kHz. Coupling and perturbing fields of similar magnitude lead to a three line transparency whereas if the perturbing field is strong it leads to a broad spectral hole with one or two absorption features at the center of the hole. Figure 9 gives the situation when the frequency of the coupling field driving the *F* transition is varied and the EIT and hole do not coincide. There is again a three line transparency although no longer symmetric. There is the impression of the hole not being affected and the EIT split into a doublet. The analysis of the observed spectrum is given below.

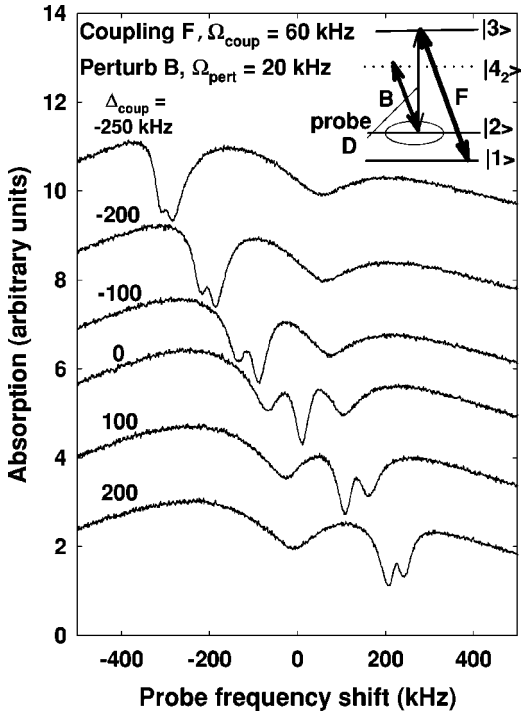

FIG. 9. Equivalent situation to Fig. 8 except the coupling frequency is varied in frequency as indicated. The zero detuning spectrum is common to Fig. 8.

VIII. PERTURBING AN EIT IN AN INHOMOGENEOUSLY BROADENED LINE: CALCULATION

The interaction of the EIT and spectral hole in Figs. 8 and 9 can be understood in terms of a regular EIT in an inhomogeneous line with some of the components in the inhomogeneous distribution no longer contributing to the spectrum. This is described in some detail. In Fig. 5, with all the lower traces contributing, a regular single transparency is obtained. If some of the centers do not contribute the line shape will be changed. For example, if the single resonant component ($\Delta_c=0$) comprising of an Autler-Townes absorption doublet, does not contribute there will be two new transparencies on either side of the central EIT. This is shown as the second top trace in Fig. 10. The three line structure becomes more pronounced when further centers symmetric about zero detuning are eliminated. This is the procedure followed in Fig. 10 and it can be seen that the resultant spectrum gives precisely the trend observed in the experimental traces of Fig. 8. Similarly if contributions from detuned centers are eliminated as done in Fig. 11 one can obtain correspondence with Fig. 9.

The above modeling of this hole burning effect where the contribution of centers are either left unchanged or totally eliminated gives a surprisingly good agreement with experi-

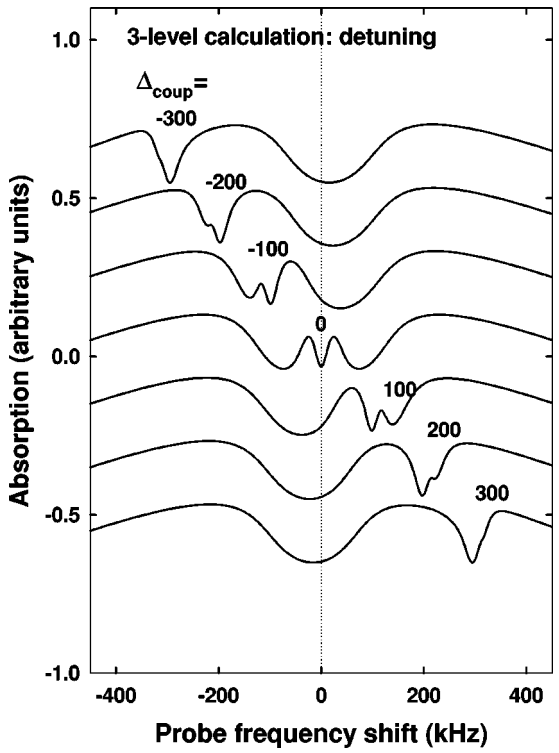

FIG. 11. Calculation of EIT in an inhomogeneous 3-level Λ system as in previous Fig. 10. Contributions from a central 100 kHz band of centers are excluded from the sum. The frequency of the coupling field is detuned as indicated such that the nominal EIT feature is displaced from zero.

ment. It is interesting to see if agreement can be obtained in a more realistic calculation.

The more formal treatment of the perturbation of an EIT involves four levels, two driving fields and a weak probe field. The density equations of motion in the rotating wave approximation for the 4-level system shown in Fig. 2(iii) have been given above and these are solved for various values of $\Omega_{coup}, \Omega_{pert}, \Delta_{coup}$, and Δ_{pert}. The parameters of the system are as given previously but are summarized in Fig. 4.

The equations are solved for individual centers within the inhomogeneous distribution and the results are shown in Fig. 12. Allowing for a Gaussian distribution the responses are added to give the predicted spectrum for an inhomogeneous line. The example in Fig. 12 is given for coupling field Rabi frequency of $\Omega_{coup}=70$ kHz and perturbing field Rabi frequency of $\Omega_{pert}=20$ kHz. In Fig. 12(i) the EIT and hole are coincident whereas in Fig. 12(ii) the EIT and hole are detuned by 100 kHz. The resultant inhomogeneous line gives a three line transparency similar to that obtained in the previous over-simplified calculation. It is also confirmed in this more complete calculation that the perturbing field indeed has little effect on most of the homogeneous components (compare Fig. 5 and Fig. 10). The resultant three line transparency arises from the decrease in the contribution from the centers near resonance (associated with spectral hole) and the more dominant contribution from off-resonance centers.

The procedure is repeated for different strengths of coupling and perturbing field. For example, in Fig. 13 a resonant coupling field of strength $\Omega_{coup}=70$ kHz is held constant and the strength of a resonant perturbing field is varied between $\Omega_{pert}=0$ and 70 kHz. The overall trend is similar to the previous calculation and the equivalent experimental variation in Fig. 8(i). The result of the calculation when the positions of the EIT and hole do not coincide is shown in Fig. 14.

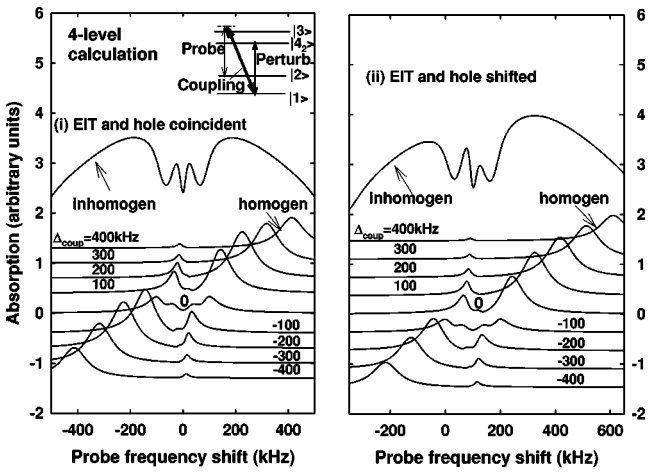

FIG. 12. Calculation of the spectrum of a 4-level system with two driving fields probed by a weak field. The levels and fields are as indicated in Fig. 4 and correspond to that obtained with EIT in a 3-level Λ system plus the probe level coupled to a fourth level. An EIT can be identified with one driving field and a hole with the second driving field. In (i) the EIT and hole are coincident whereas in (ii) the frequency of the field inducing the EIT is detuned by 100 kHz. The lower traces in each case give the spectrum of homogeneous components whereas the upper trace gives the resultant inhomogeneously broadened spectrum. The spectrum is obtained with $\Omega_{coup}=70$ kHz and $\Omega_{pert}=25$ kHz.

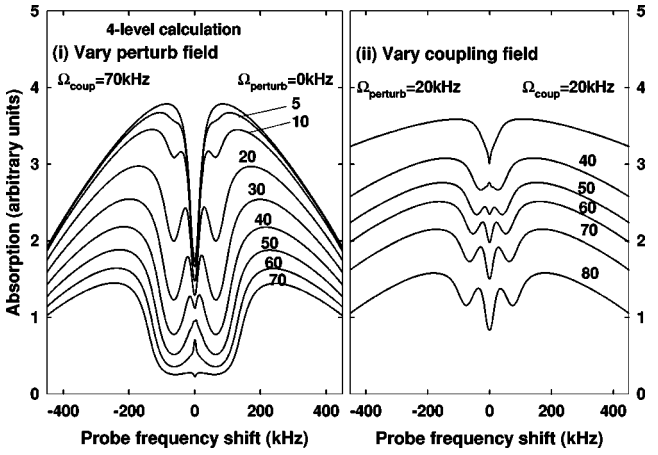

FIG. 13. The calculation of the spectrum of an inhomogeneous broadened 4-level system driven by two fields and probed by a weak-field following approach shown in Fig. 12. The spectra can be compared with experimental traces in Fig. 8. In (i) the inhomogeneous spectrum is shown for a fixed coupling field $\Omega_{coup}=70$ kHz whereas the strength of the perturbing field is varied as indicated. In (ii) the perturbing field is fixed at $\Omega_{pert}=20$ kHz and coupling field is varied as indicated.

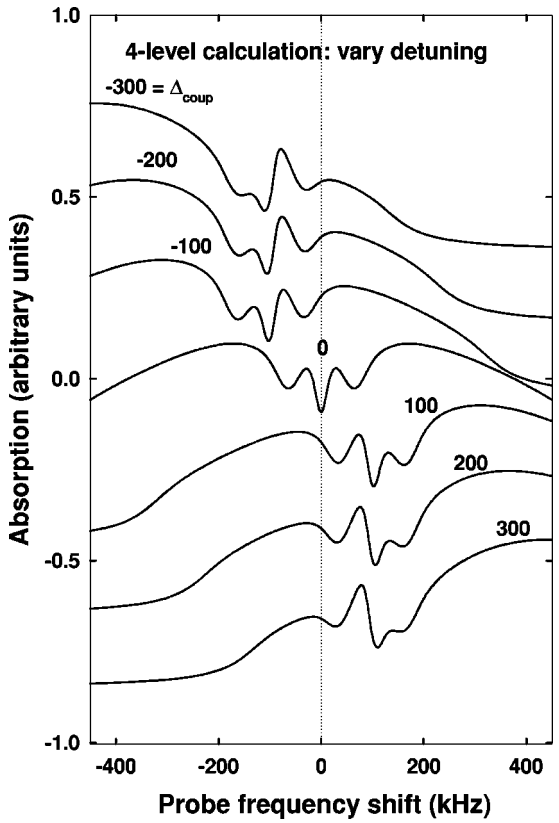

FIG. 14. Calculation of the spectrum of an inhomogeneously broadened 4-level system driven by two fields and probed by a weak-field corresponding to the experimental situation in Fig. 9(ii). The coupling field $\Omega_{coup}=70$ kHz and perturbing field $\Omega_{pert}=40$ kHz are fixed in strength but the frequency of the coupling field is varied in steps of 100 kHz.

IX. DISCUSSION

Both the simplified 3-level and 4-level calculations account for the major trends in the experimental spectra. For example, for the case where the EIT and hole are coincident Fig. 10 and Fig. 13 should be compared with Fig. 8 and for the detuned case Fig. 11 and Fig. 14 with Fig. 9. The comparison is mainly qualitative but the agreements are reasonable.

There are only minor differences between the results of the 3- and 4-level calculations and the reason for the similarity is worth considering. A strong driving field can certainly split a probed transition with a shared level. In the 3-level case this is seen as an Autler-Townes splitting in the resonant case with $\Delta=0$ in Fig. 5. When a strong driving field is added to a fourth level from a dressed state analysis four lines can be expected in the spectrum and is shown for the resonant case in Fig. 12. Therefore, as two lines are expected for the 3-level system and four for the 4-level system clearly the difference are substantial. However, in the 3-level case the resonant trace is not included in the calculation of the perturbed inhomogeneous line and in the 4-level case the four peaked structure is weak and makes little contribution. For off-resonance fields the situation is different. For a 4-level calculation there are still four features but two of the features become weak and the spectra approaches that of the 3-level case (compare Fig. 5 and Fig. 12). In short there are differences in the calculation for 3- and 4-level systems but the inhomogeneous spectra is totally dominated by off-resonant centers for which the spectra are almost the same.

The agreement with experiment is only moderate in the case when there is a detuning between the frequency of the hole and that of the EIT. For example, the results of the 4-level calculation given in Fig. 14 are in poor correspondence with the experimental traces in Fig. 9. The 3-level calculation is more satisfactory. The reason for the poorer correspondence in the case of the 4-level calculation (Fig. 14 compared with Fig. 9) is not well understood. It could be that there is a loss of population to other spin levels and the closed 4-level model will not allow for this effect. A reduced contribution is precisely the approach in the 3-level calculation and would account for better agreement.

With strong perturbing fields there is a small but significant difference between the spectrum obtained for the 4-level and 3-level calculations near zero detuning [lowest trace in Fig. 10 and Fig. 13(i)]. One absorption in the 4-level calculation and two in the 3-level case. The features arise from an induced absorption associated with positively and negatively detuned centers. The peaks are displaced from the minimum absorption (see Fig. 6 of Ref. [1]) and, hence, the induced absorption peaks are on either side of zero detuning. This displacement can be interpreted in terms of ''light shift.'' However, any equivalent light shift associated with the perturbing field is neglected in the 3-level calculation but included in the 4-level calculation. When included the shifts are in the opposite sense and when the two fields are equivalent (occurring as the parameters are similar when the fields are near equal) the peaks coincide to give a single line. The single feature with a linewidth of 33 kHz is predicted in rough correspondence with the experimental value of 22 kHz. The inaccuracy in the linewidth and gain rather than absorption is presumably due to approximations made in choosing the parameters. The significance is that the more appropriate 4-level calculation correctly predicts the single sharp absorption at zero detuning observed in the experimental trace Fig. 8(i).

Another feature worth noting is the rectangular nature of the spectral hole. A rectangular hole is obtained in the case of saturating a 2-level system when T_2 approaches T_1 [21] and this is the case here. The relaxation is determined by the optical pumping cycle and we have reported $T_2=0.4\ T_1$ for a similar experimental situation [16]. The rectangular nature of the hole is only weakly susceptible to the precise T_2/T_1 ratio and we have chosen $T_2=T_1$.

The experiments give the first observation of perturbed EIT in a solid state system and the main aim of the study has been to identify the physical origin of the changes to the EIT features. For this it is satisfactory to use fairly generalized parameters. For example, we have used only one electron-spin dephasing of 60 kHz and one for hyperfine dephasing of 10 kHz. The results of the calculations will indicate the trends of a perturbed spectrum and these are in general agreement with the observations. Better agreement might be obtained if we established the parameters under the precise experimental conditions. However, it should be realized that

the models are very much simpler than the real system. There are in fact nine spin levels (Fig. 1), or twenty seven if we included the optical levels, and this is being approximate by 4 levels. It is not, therefore, clear that more precise parameters within models used will be more satisfactory. The present correspondence is certainly adequate to firmly establish the origin of the spectral variation.

X. CONCLUSIONS

In summary, we have investigated how EIT in a Λ scheme is affected by an additional electromagnetic field. There are three cases depending on which of the three levels in the Λ system is affected by the extra field. The experimental measurements are for an inhomogeneously broadened transitions and for two of the three cases the inhomogeneous broadening is an important factor. The case where the extra field perturbs the shared level, the inhomogeneous broadening is not an issue and in effect the spectrum is the same as for a homogeneously broadened system. In fact the perturbing field does not affect the EIT in first order. However, in the other two cases the EIT is affected and the inhomogeneous broadening totally changes the response compared with that expected for a homogeneously broadened system. For example, when the coupling level is effected in a homogeneously broadened case a three line absorption is expected but the EIT is lost when the system is inhomogeneous broadened.

The last case is much more interesting and has been the focus for much of the paper. This is where the new field directly affects the probed level of the Λ system. The effect of the perturbing field is to cause spectral hole burning and the hole ''interferes'' with the EIT. Some centers within the inhomogeneous line no longer contribute and the result is a complex spectrum but readily interpreted when allowing for the reduced contributions. It should also be realized that similar line shapes could arise in other situations in solids. For example, should strain produce an irregular inhomogeneous line shape the EIT in a nonsymmetric line will give an irregular EIT line shape. Depending on the strain distribution the EIT feature will be distorted or split. It follows the EIT line shape in Gaussian and Lorenzian lines will be different.

The present studies are of spin levels in a solid at radio frequencies but the system has many characteristics of an optical system. For example, accepting the difference in scale, there are inhomogeneously broadened transitions between well separated electron-spin levels. These are analogous to optical transitions. The spin transitions have resolved structure associated with the hyperfine levels analogous to optical transitions to the different levels of a multiplet. Also what makes this electron-spin system unique is that the population is predominantly in the lowest level and this is similar to an optical system at low temperatures. There are, therefore, many parallels with optical systems and the present studies will be useful in anticipating worthwhile experiments at optical frequencies where the sources are not so readily available. Perturbation of EIT at optical frequencies in solids have not been reported but the present observation will help in the planning of such experiments. The situation of gases is also not substantially different and the observation will provide guidance to the effects obtainable with Doppler broaden atomic transitions.

[1] G. Orriolis II, Nuovo Cimento Soc. Ital. Fis., B **53B**, 1 (1979).
[2] S.E. Harris, Phys. Today **50**(7), 36 (1997).
[3] E. Arimondo, *Prog. in Optics XXXV*, edited by E. Wolf (North-Holland, Amsderdam, 1996), pp 259–354.
[4] C. Wei and N.B. Manson, J. Opt. B: Quantum Semiclassical Opt. **1**, 464 (1999).
[5] N.B. Manson, P.T.H. Fisk, and X.-F. He, Appl. Magn. Reson. **3**, 999 (1992).
[6] O. Kocharovskaya, Phys. Rep. **219**, 175 (1992); M.O. Scully, *ibid.* **219**, 191 (1992).
[7] K.M. Gheri, P. Grangier, J-P. Poizat, and D.F. Walls, Phys. Rev. A **46**, 4276 (1992).
[8] L.V. Hau, S.E. Harris, Z. Dutton, and C.H. Behroozi, Nature (London) **397**, 594 (1999); M.M. Kash, V.A. Sautenkov, A.S. Zibrov, L. Hollberg, G.R. Welch, M.D. Lukin, Y. Rostovtsev, E.S. Fry, and M.O. Scully, Phys. Rev. Lett. **82**, 5229 (1999).
[9] S.E. Harris, J.E. Field, and A. Imamoğlu, Phys. Rev. Lett. **64**, 1107 (1990).
[10] M.D. Lukin, S.F. Yelin, M. Fleischhauer, and M.O. Scully, Phys. Rev. A **60**, 3225 (1999).
[11] G. Davies and M.F. Hamer, Proc. R. Soc. London, Ser. A 285 (1976).
[12] Y. Mita, Phys. Rev. B **53**, 11 360 (1996).
[13] van Wyke and Loubser, Diamond Res. **4**, 11 (1977).
[14] N.R.S. Reddy, N.B. Manson, and E. R Krausz, J. Lumin. **38**, 46 (1987).
[15] J. Mlynek, N.C. Wong, R.G. DeVoe, E.S. Kintzer, and R.G. Brewer, Phys. Rev. Lett. **50**, 993 (1983); N.C. Wong, E.S. Kintzer, J. Mlynek, R.G. DeVoe, and R.G. Brewer, Phys. Rev. B **28**, 4993 (1983).
[16] S.A. Holmstrom, C. Wei, A.S.M. Windsor, N.B. Manson, J.P.D. Martin, and M. Glasbeek, Phys. Rev. Lett. **78**, 302 (1997).
[17] C. Wei, D. Suter, A.S.M. Windsor, and N.B. Manson, Phys. Rev. A **58**, 2310 (1998).
[18] S.R. de Echaniz, A.D. Greentree, A.V. Durrant, D.M. Segal, J.P. Marangos, and J. A Vaccaro, Phys. Rev. A **64**, 013812 (2001).
[19] C.Y. Ye, A.S. Zibrov, and Yu.V. Rostovtsev, J. Mod. Opt. **49**, 391 (2002).
[20] C. Wei and N.B. Manson, Phys. Rev. A **60**, 2540 (1999).
[21] R.N. Shakhmuratov and R.A. Khasanshin, [Opt. Spectrosc. **79**, 340 (1995)].